

Water hammer investigation of shut-down of high-head hydropower plant at very high Reynolds number flows

Uroš Karadžić^{1,*} - Anton Bergant^{2,3} - Danica Starinac⁴ - Boško Božović⁵

¹University of Montenegro, Podgorica, Montenegro

²Litostroj Power d.o.o., Ljubljana, Slovenia (Full-Time), ³University of Ljubljana, Ljubljana, Slovenia (Part-Time)

⁴Jaroslav Černi Institute, Belgrade, Serbia

⁵Electric Power Supply Company, Nikšić, Montenegro

This paper investigates water hammer phenomena in a refurbished high-head hydropower plant Perućica, Montenegro during shut-down of the entire plant – simultaneous closure of the seven Pelton turbine units. In-situ measuring campaign during a number of steady and unsteady conditions has been performed on the plant's open channel, pressurized and tail race sub-systems with primarily goal to define measures that will enable achievement of the plant's installed capacity. In-house software written in Visual Fortran and based on the method of characteristics (MOC) has been developed. Closure of the Pelton turbine distributors is modelled by the two-speed closing law. Dissipation torques in turbine housing and shaft bearings are considered in calculation of the Pelton turbine unit rotational speed change. Numerical results given for standard quasi-steady and convolution based unsteady friction model are compared with results of measurements at flows with very high initial Reynolds numbers (larger than 10^7). Developed numerical model shows good agreement with the results of site measurements. It is shown that the unsteady friction has a small impact on pressure histories in Perućica HPP.

Keywords: water hammer, high-head hydropower plant, Pelton turbine, emergency shut-down, high Reynolds number

Highlights:

- Water hammer during emergency shut-down of the high-head hydropower plant is investigated.
- Numerical model based on the method of characteristics is developed.
- Verification of numerical model is done by comparison of measurements that have been made at the entire plant system.
- Pressure histories at the downstream end of three parallel penstocks, penstock inlet valve chambers, surge tank as well as turbine speed changes are investigated and commented.
- Influence of unsteady friction is of minor importance for relatively slow transients considered at initially high Reynolds numbers (larger than 10^7).

0 INTRODUCTION

Water hammer in hydropower plants (HPPs) is caused by closing or opening of the turbine unit distributors, operation of the safety shutoff valves as well as unwanted turbine runaway. Careful water hammer control is essential in order to ensure reliable operation of hydropower plants. If this is not provided severe problems may arise in operation, damage of individual components of the system may occur or, in the worst case, accidents with human casualties may happen [1] to [5]. Modelling and

analysis of extreme hydraulic transients (plant emergency shut-down) in new or refurbished HPPs are of utmost importance because in this way extreme values of pressures that may occur during system exploitation can be determined. Based on these values, closing and opening times of the turbine units' distributors are devised as well as dimensioning of the system components is done.

The objective of this paper is to investigate and discuss water hammer effects in Perućica HPP, Montenegro during the entire plant emergency shut-down i.e. simultaneous closure of

*Corr. Author's Address: University of Montenegro, Faculty of Mechanical Engineering, Džordža Vasiingtona nn, 81000 Podgorica, Montenegro, uros.karadzic@ucg.ac.me

all seven Pelton turbine units. The units are installed in three parallel penstocks (each of about 2 km long) that are coupled to a concrete tunnel (about 3.3 km long) with a surge tank. Previously, measurements of one and two Pelton turbines in one penstock only have been investigated [6]. This paper presents new results at much higher Reynolds number flows (higher than 10^7) than previously (in order of 10^6).

In the first part of the paper mathematical tools for solving water hammer equations are presented [7], [8]. Friction losses in the plant's penstocks are calculated with two different models: (1) standard quasi-steady (QSF) and (2) convolution-based unsteady friction model (CBM) [9], [10]. Turbine speed change during emergency shut-down is calculated taking into account dissipative torques including the shaft bearing friction torque and ventilation losses in the turbine housing [6]. In the second part of the paper comparisons of numerical and field test results are made for the case of the entire plant shut-down. Results given for pressure changes in plant's penstocks, feeding tunnel as well as water level fluctuations in surge tank and turbine speed change are investigated and commented.

1 THEORETICAL MODELLING

Water hammer refers to the transmission of pressure waves in liquid-filled pipelines resulting from a change in flow velocity. For most engineering applications simplified water hammer equations neglecting the convective terms are used in analysis [7], [8].

$$\frac{\partial H}{\partial t} + \frac{a^2}{gA} \frac{\partial Q}{\partial x} = 0, \quad (1)$$

$$\frac{\partial H}{\partial x} + \frac{1}{gA} \frac{\partial Q}{\partial t} + \frac{fQ|Q|}{2gDA^2} = 0, \quad (2)$$

where, H = piezometric head (head), t = time, a = pressure wave speed, g = gravitational acceleration, A = pipe area, Q = discharge, x = axial co-ordinate, f = Darcy-Weisbach friction factor, and D = pipe diameter. All the symbols are defined as they appear first in the paper. For solving Eqs. (1) and (2) the staggered (diamond) grid [7] in applying the method of characteristics is used in this paper.

1.1 Friction Losses

For evaluation of friction factor in Eq. (2) the standard quasi-steady approach is traditionally used. This model does not give good results for fast transients and it is shown that inclusion of unsteady friction significantly improves numerical results [11], [12]. Up to date a little is published about unsteady friction effects in real hydro systems [6], [13]. Duan et al. [14] investigated the relative importance of unsteady friction in the pipelines taking into account pipe size and length. They introduced dimensionless parameter $I_D = fV_0L/(aD)$ and concluded that the effects of unsteady friction for fast transients (sudden and complete valve closure) are important when $I_D < 0.10$. However, unsteady friction may be important in some cases such as behavior close to resonance. In case of plant emergency shut-down unsteady friction has to be investigated and included into numerical model since it is shown that the model with unsteady friction included gives some higher values of maximum system's pressure than QSF model [6]. The friction factor f can be expressed as the sum of the quasi-steady part f_q and the unsteady part f_u [15], [16],

$$f = f_q + f_u. \quad (3)$$

The quasi-steady friction factor is calculated and updated every time step according to standard formulae for evaluating quasi-steady friction losses. For determination of unsteady friction factor a convolution-based model (CBM) is used for simulation in this paper [9]. The traditional implementation of CBM in the MOC results in many convolution calculations that increase the computational time dramatically. However, the computationally efficient unsteady friction factor can be defined by using approximated weighting functions embedded in a finite sum of N_k functions $y_k(t)$ as originally proposed by Trikha [17] in his three-function approximation of Zielke's weighting function for transient laminar flow,

$$f_u = \frac{32\nu A}{DQ|Q|} \sum_{k=1}^{N_k} y_k(t). \quad (4)$$

A number of authors have developed multi-function approximations with a lesser or higher degree of accuracy. Approximations have been developed for original Zielke's weighting function for transient laminar flow and numerous weighting functions for transient turbulent flow [10], [18], [19]. The widely used Vítkovský et al. approximation [20] is accurate over a broad range of dimensionless times $\Delta\tau = \Delta t 4 \nu / D^2$ [10^{-6} , 10^{-1}]. For lower $\Delta\tau$ values Urbanowicz [21], [22] developed a computationally efficient and

accurate approximation of weighting functions that should be used when $\Delta\tau \leq 10^{-6}$.

1.2 Pelton turbine model

Pelton turbine output is regulated by control of discharge that acts on the turbine wheel. Discharge is adjusted by closing or opening the nozzle throat by means of a needle (Fig. 1) and with an appropriate position of the jet deflector.

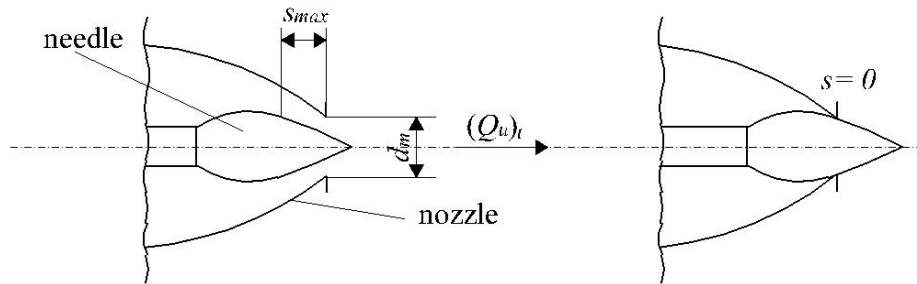


Fig. 1. Pelton turbine distributor (needle valve)

The discharge through the nozzle is only dependent on the position of the needle valve and it does not depend on the turbine unit rotational speed as is the case in reaction water turbines. Therefore, the water hammer equations and the dynamic equation of the unit rotating parts can be solved separately. In this way the instantaneous head at the nozzle inlet and instantaneous discharge through the nozzle are calculated by the MOC and these values are used as an input in the solution method for the dynamic equation of the unit rotating parts. The instantaneous discharge through the nozzle ($(Q_u)_t$) is determined from the following relation [6],

$$(Q_u)_t = K_Q A_m \sqrt{2g(H_{u,t} - H_d)} \quad (5)$$

where, K_Q is nozzle discharge coefficient, A_m is nozzle area ($A_m = \pi d_m^2 / 4$), d_m is nozzle diameter, $H_{u,t}$ is the instantaneous head at the nozzle inlet, and $H_d = const.$ is head downstream the nozzle. The nozzle discharge coefficient is function of the nozzle opening. The needle closing law is expressed as,

$$s = \tau \cdot s_{max} \quad (6)$$

where, τ = dimensionless nozzle opening and s_{max} = maximum needle stroke. The procedure for calculating needle closing run is described in detail in [6].

The emergency shut-down of the turbine unit is the most severe normal operating transient regime [8]. The turbine is disconnected from the electrical grid followed by simultaneous gradual full-closure of the needle(s) and rapid activation of the jet deflector(s). The equation that describes dynamic behaviour of the Pelton turbine unit rotating parts during emergency shut-down is [6],

$$T_a \frac{d\varphi}{dt} = m_h - m_{fr} - m_{air} \quad (7)$$

where, T_a is the mechanical starting time [8], $\varphi = (n - n_r) / n_r$ is relative speed change, n is turbine rotational speed (traditionally in rpm), r defines rated conditions, m_h is dimensionless hydraulic torque, m_{fr} is dimensionless shaft bearing friction torque, and m_{air} is dimensionless fluid damping torque (ventilation losses in the turbine housing) – see [6] for details. Equation (7) can be solved analytically [6].

1.3 Note on other boundary conditions

Theoretical models for the reservoirs, orifice type surge tank and branching junction (trifurcation)

2 PERUĆICA FLOW-PASSAGE SYSTEM

Perućica HPP was built in the mid fifties of 20th century. The flow-passage system (Fig. 2) is a complex system comprised of intake structure with guard gate, concrete tunnel (length $L_T = 3335$ m, diameter $D_T = 4.8$ m), orifice type surge tank (orifice head loss coefficients: $\zeta_{in} = 1.65$ and $\zeta_{out} = 2.48$ during inflow and outflow, respectively) of cylindrical cross-section ($D_{ST} =$

can be found in standard water hammer textbooks [7], [8].

8.0 m) with an expansion at elevation $z = 611.0$ m ($D_{ST} = 12.0$ m) and overflow (elevation: $z_{ov} = 628.0$ m; width of the overflow weir: $b_{ov} = 7.98$ m with discharge coefficient $\mu_{ov} = 0.4$) and three parallel steel penstocks (Fig. 3a) with horizontal-shaft twin type Pelton turbines built at their downstream ends (Fig. 3b).

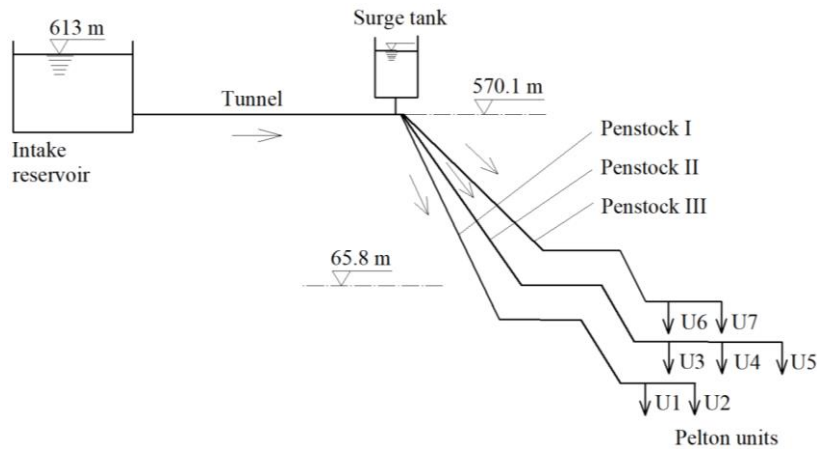


Fig. 2. Layout of Perućica HPP, Montenegro

The equivalent length and diameter [8] of penstock *I* are 1920 m and 1.96 m, respectively; for penstock *II* 1966 m and 2.16 m; for penstock *III* 2014 m and 2.57 m. The penstock *I* feeds two turbine units (U1 and U2) with rated unit power of 39 MW, penstock *II* feeds three turbine units (U3, U4 and U5) of 39 MW each and penstock *III* feeds two units (U6 and U7) of 59 MW each. The

distributors of the first four units (U1 to U4) have been already refurbished. The maximum water level at the intake is 613 m and the minimum one is 602.5 m. The Pelton wheel diameter of units U1 to U5 is $D_k = 2400$ mm and for units U6 and U7 is $D_k = 2100$ mm. The rotational speed of U1 to U5 is $n = 375$ min^{-1} , and of U6 and U7 is $n = 428$ min^{-1} .

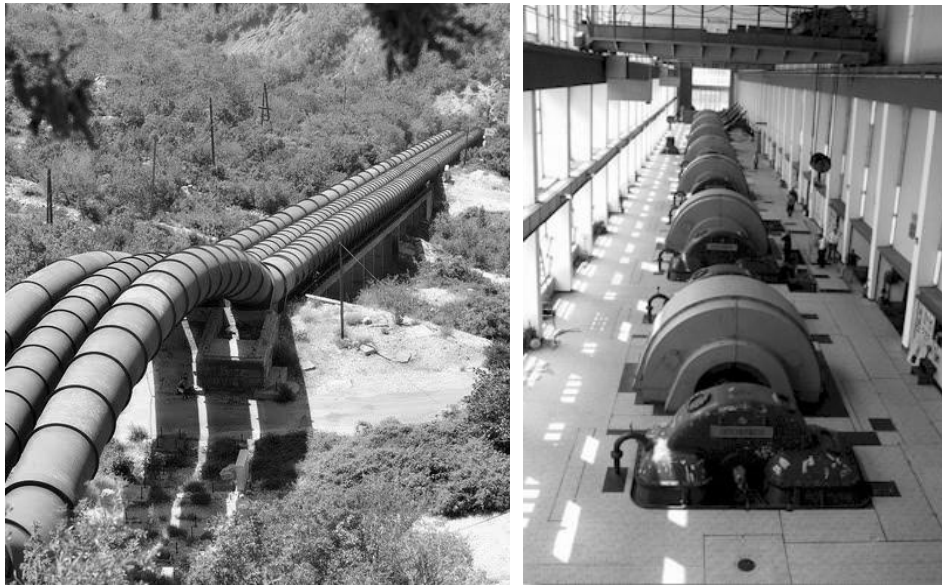


Fig. 3. Layout of a) three parallel penstocks and b) powerhouse with seven twin type Pelton units in Perućica HPP

2.1 Instrumentation

Recently, the Hydraulic Department of the Jaroslav Černi Institute, Belgrade, Serbia, has performed comprehensive in-situ measurements (water levels, discharges, pressures, displacements, stresses and vibrations) at different locations throughout the entire HPP system. Numerous steady-state and unsteady state scenarios have been tested, through continuous and simultaneous measurements at all measurement stations including intake structure (feeding channels and reservoir), tunnel with surge tank, three parallel penstocks with seven Pelton turbine units and outlet structure [23], [24]. During shut-down of the entire power plant all influential quantities were continuously measured including pressures at the inlet of the turbines, strokes of the needles and of the jet deflectors, units' rotational speeds, pressures at the downstream end of the tunnel and the upstream end of the penstocks (penstock valve chambers) as well as water level in the surge tank. Pressures at the upstream end of the distributors were measured by absolute high-pressure piezoresistive transducers *Cerabar T PMP 131-A1101A70 Endress+Hauser* (pressure range 0 to 100 bar, uncertainty in measurement ± 0.5 %).

Pressures at the valve chamber were measured by absolute high-pressure piezoresistive transducers *Cerabar T PMP 131-A1101A70 Endress+Hauser* (pressure range 0 to 10 bar, uncertainty in measurement ± 0.5 %). The needle stroke and the stroke of the jet deflector were measured by displacement transducers *Balluff BTL5-S112-M0175-B-532* and *Balluff BTL5-S112-M0275-B-532*, respectively. Uncertainty of these sensors is ± 0.03 mm. The turbine rotational speed was measured using inductive sensor *Balluff BES M18MI-PSC50B-S04K* (uncertainty in measurement ± 0.03 %). The surge tank water level was measured by radar sensor *Micropilot M FMR240 Endress+Hauser* (range 0 to 70 m, uncertainty in measurement ± 3 mm). The initial discharges in the penstocks were measured by ultrasonic flowmeters *Prosonic Flow 93W, Endress+Hauser* (velocity range up to 15 m/s, uncertainty in measurements ± 0.5 %).

3 COMPARISON OF NUMERICAL AND IN-SITU TEST RESULTS

During the campaign the following steady and unsteady regimes were investigated: the unit start-up and stop, load acceptance and reduction, load rejection under governor control and

emergency shut-down, and closure of turbine safety valves against the discharge.

In this paper the simultaneous emergency shut-down of all seven Pelton turbine units is investigated. Total initial power output of the plant was 303.54 MW and discharge in the feeding tunnel was $Q_T = 70.24 \text{ m}^3/\text{s}$. The measured needle closing times and initial opening of the nozzles are presented in Table 1. Initial capacities and discharges per unit are shown in Table 2 where initial unit's discharges were calculated from known initial capacity (plant SCADA system), measured net head and measured initial opening of the nozzles. Measured initial discharges in the penstocks were $Q_I = 17.4 \text{ m}^3/\text{s}$, $Q_{II} = 25.38 \text{ m}^3/\text{s}$, $Q_{III} = 27.46 \text{ m}^3/\text{s}$, respectively. Flows in the feeding tunnel and penstocks were turbulent with large Reynolds numbers, $Re_T = 1.86 \times 10^7$, $Re_I = 1.13 \times 10^7$, $Re_{II} = 1.5 \times 10^7$ and $Re_{III} = 1.36 \times 10^7$. Initial steady friction factors in tunnel and penstocks are $f_{0T} = 0.0146$, $f_{0I} = 0.0105$, $f_{0II} = 0.0118$ and $f_{0III} = 0.0152$. The water level at the intake was $z_R =$

603.6 m. Estimated pressure wave speeds in tunnel and three penstocks are $a_T = 1354 \text{ m/s}$, $a_I = 1148 \text{ m/s}$, $a_{II} = 1123 \text{ m/s}$ and $a_{III} = 1152 \text{ m/s}$, respectively [6]. Basic time step in the staggered grid MOC code was $\Delta t = 0.04 \text{ s}$. Numerical results obtained from the standard quasi-steady friction model (QSF) and the convolution based unsteady friction model (CBM) are compared with the results of measurements. Dimensionless times used in CBM (see Section 1.1) for the tunnel, and penstocks *I*, *II* and *III* are $\Delta\tau = \{0.0069 \times 10^{-6}, 0.0414 \times 10^{-6}, 0.0342 \times 10^{-6}, 0.0242 \times 10^{-6}\}$, respectively. Consequently, the Urbanowicz approximation model in CBM [21], [22] has been used. Duan's parameter [14] for the tunnel and three penstocks is $I_D = \{0.014, 0.0834, 0.0847, 0.03\}$. The needle valve closure times are slow (see Table 1) and Duan's parameter cannot be used for this case. However, there is a need to extend Duan's parameter for cases with slower valve closure times ($0 < t_c \leq 2L/a$, $t_c > 2L/a$, $t_c > 10L/a$).

Table 1. Needle valve closing times and initial opening of the nozzles

Unit and needle	Closing time (s)	Nozzle opening (%)	Nozzle opening s_0 (mm)
U1n _a	71.5	88.77	133.2
U1n _b	70.0	88.77	133.2
U2n _a	73.5	90.62	135.9
U2n _b	70.0	90.62	135.9
U3n _a	49.0	90.52	135.8
U3n _b	44.0	90.52	135.8
U4n _a	70.0	94.17	141.2
U4n _b	67.0	94.17	141.2
U5n _a	40.0	86.0	167.7
U5n _b	48.0	86.0	167.7
U6n _a	108.5	99.42	165.0
U6n _b	86.0	99.55	165.2
U6n _c	114.0	99.58	165.3
U6n _d	95.0	99.65	165.4
U7n _a	95.0	96.88	160.8
U7n _b	67.5	97.12	161.2
U7n _c	116.5	97.12	161.2
U7n _d	69.0	97.12	161.2

Table 2. The initial unit's powers and discharges

	U1	U2	U3	U4	U5	U6	U7	Total
P (MW)	37.9	37.7	36.9	37.3	38	59.1	56.6	303.54
Q (m ³ /s)	8.65	8.75	8.64	8.74	8.0	13.8	13.66	70.24

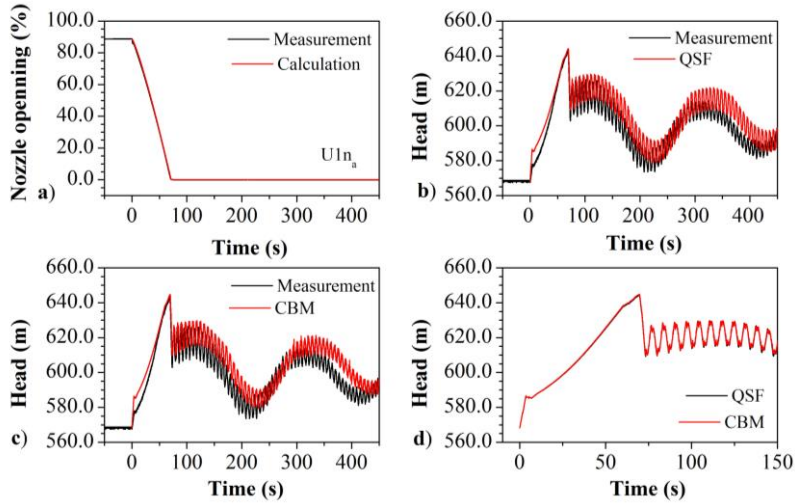


Fig. 4. Comparison of piezometric heads (heads) and needle stroke (s) at the end of penstock I (datum level $z = 0.0$ m; time step $\Delta t = 0.04$ s).

Comparison of calculated and measured heads at the downstream end of penstock I and needle strokes is shown in Fig. 4. The maximum measured head is obtained at the end of nozzle closure process and it is 643.5 m with head rise of 75.1 m. The maximum heads obtained by numerical models have some higher values and are equal to 644 m (QSF, Fig 4b) and 644.6 m (CBM, Fig 4c). All maximum head values are below the maximum permissible system head of 668 m. The closing time is much larger than the water hammer reflection time of $2L_1/a_1 = 3.34$ s. It should be noted that, in the event of unit shut-down from smaller initial powers, the closing

time of the nozzles can be within water hammer reflection time, which can cause an unacceptable head increase. Special attention should be paid to this problem [25]. After nozzles are closed numerical models give some higher head values but, generally, they are in good agreement with results of the measurements. The results obtained by QSF and CBM numerical models are practically the same in the first 150 s of transient processes (Fig. 4d) and after that time CBM model better attenuates pressure waves and gives results that are closer to the measurements (Figs. 4b and 4c).

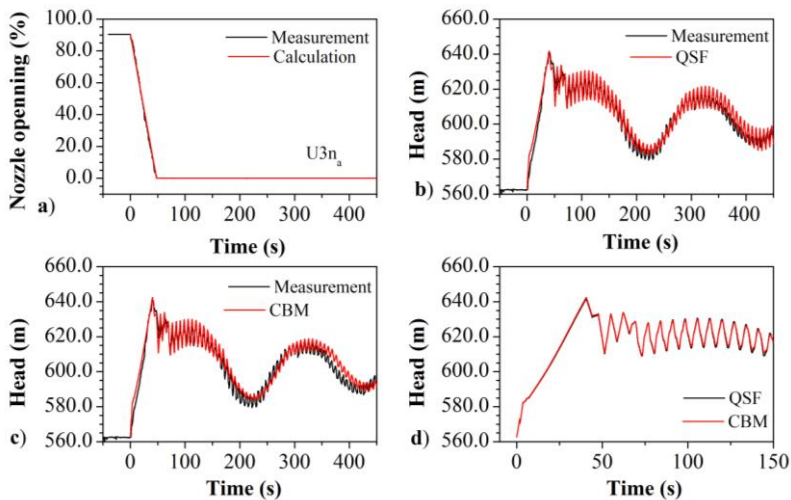


Fig. 5. Comparison of piezometric heads (heads) and needle stroke (s) at the end of penstock II (datum level $z = 0.0$ m; time step $\Delta t = 0.04$ s).

Fig. 5 shows comparison of measured and calculated heads and needle strokes at the downstream end of penstock *II*. Like in the penstock *I*, the maximum head occurs after the nozzles were closed and it is 641.0 m with a head increase of 78.6 m. The maximum head values obtained by QSF and CBM numerical models are in a good agreement with measured values and they are 641.5 m and 642.0 m, respectively (Figs.

5b and 5c). Calculated and measured values are below the maximum system allowed head of 668 m. The closing time, like in the penstock *I*, is much larger than the water hammer reflection time of $2L_{II}/a_{II} = 3.5$ s. Numerical results show good agreement with measured results during entire transient period with the CBM results slightly closer to the measured results (Figs. 5b and 5c).

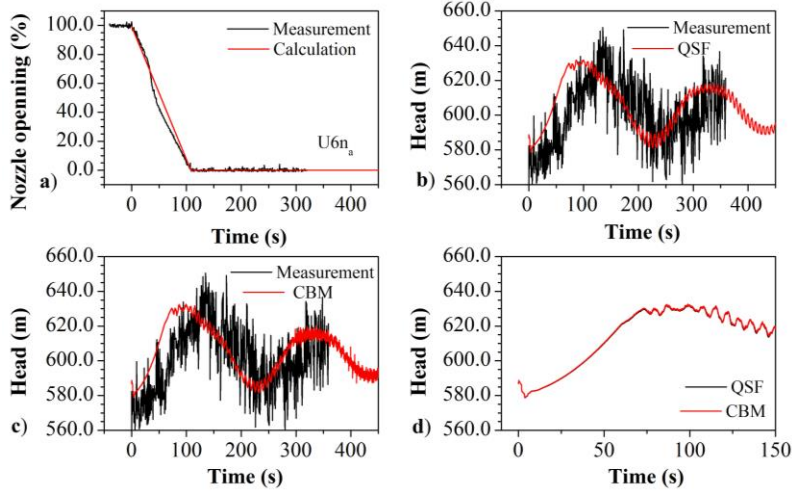


Fig. 6. Comparison of piezometric heads (heads) and needle stroke (s) at the end of penstock *III* (datum level $z = 0.0$ m; time step $\Delta t = 0.04$ s).

Fig. 6 shows comparisons of heads and needle strokes at the downstream end of penstock *III*. Unfortunately, during experiment the pressure transducer installed at the downstream end of the penstock *III* has been broken down; however, the magnitude and shape of measured pressure head histories follow the same path as calculated ones (Figs. 6b and 6c). The head increase in penstock *III* obtained by QSF model is 44.1 m and by CBM model is 45.1 m. The maximum head value given by QSF is 631 m at time $t = 100.0$ s where the value of maximum head by CBM model is 632 m also at time $t = 100.0$ s. It should be noted that in penstock *III* eight nozzles were closed from which the first was closed at $t = 67.5$ s ($U7n_b$) and the last at $t = 116.5$ s ($U7n_c$). In this period uneven head oscillations occurred (Fig. 6d). The pressure wave travels to the surge tank and back and found nozzles with different degree of opening every time. Consequently, the

discharge between the units 6 and 7 is not evenly divided over the duration of the transient process. The similar situation occurred also in the penstock *II* (Fig. 5d). The water hammer reflection time of penstock *III* is equal to water hammer reflection time of penstock *II* i.e. $2L_{III}/a_{III} = 3.5$ s. It is planned to refurbish distributors of units *U5* to *U7* and their governors. Then the closing time of all nozzles on all units will finally be adjusted so that the nozzles on the individual penstocks have the same closing times. It should be noted that, according to original project documentation, closing times for all nozzles for the case of the entire plant shut-down are equal to 80 s.

Let us now examine pressure head histories at the branching junction that connects downstream end of the tunnel and upstream end of the three parallel penstocks (Fig. 2). Surge tank is located 85 m upstream of the junction. The measured and calculated head changes at the downstream end of the concrete tunnel and the

upstream end of the three steel penstocks are shown in Figs. 7 and 8.

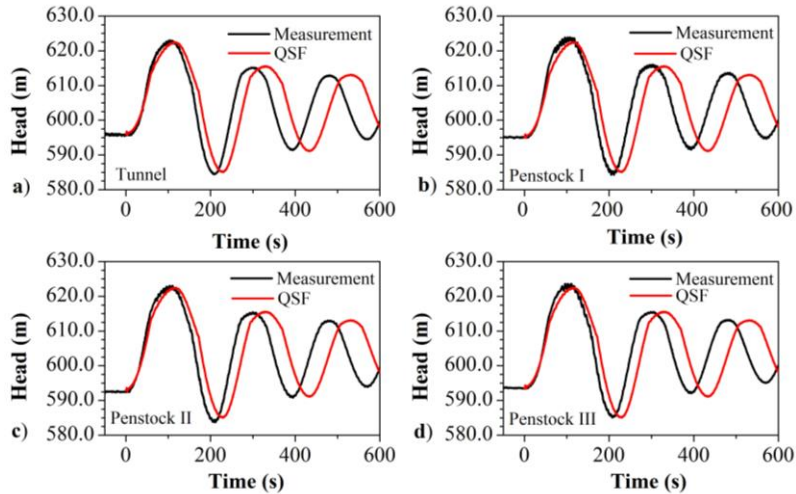


Fig. 7. Comparison of piezometric heads (heads) at the valve chamber (QSF model; datum level $z = 0.0$ m; time step $\Delta t = 0.04$ s).

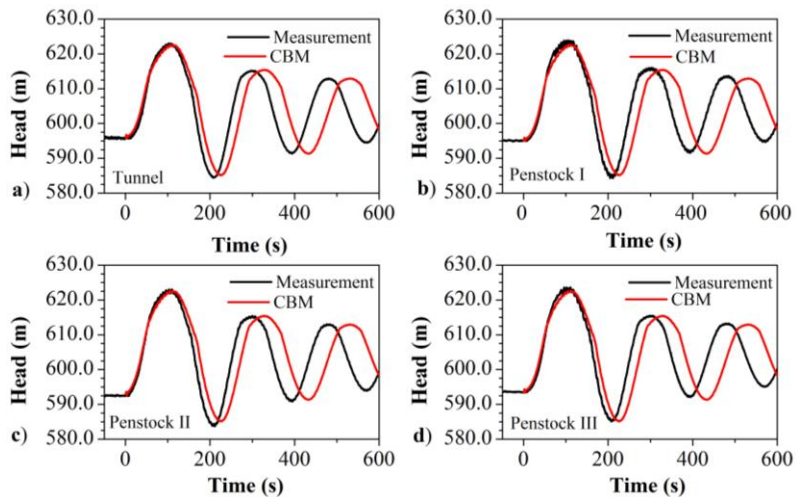


Fig. 8. Comparison of piezometric heads (heads) at the valve chamber (CBM model; datum level $z = 0.0$ m; time step $\Delta t = 0.04$ s).

The maximum measured heads are: 622.8 m (tunnel, Fig. 7a), 623.7 m (penstock I, Fig. 7b), 622.9 m (penstock II, Fig. 7c) and 623.5 m (penstock III, Fig. 7d). Minimum measured heads in the valve chambers are: 584.5 m (tunnel), 584.4 m (penstock I), 583.8 m (penstock

II) and 585.1 m (penstock III). QSF and CBM give practically the same results with the maximum and minimum head values close to measured one (Figs. 7 and 8). However, there is a phase shift which increases during the time.

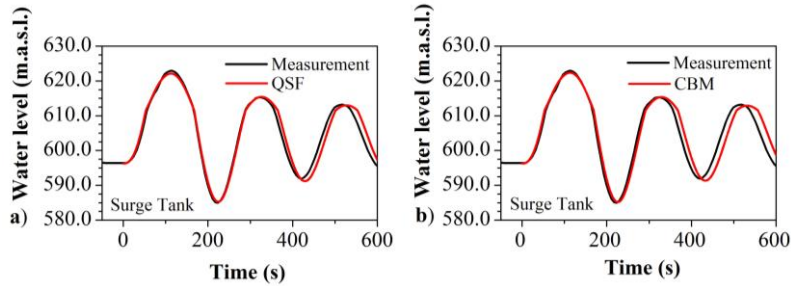


Fig. 9. Comparison of water level in the surge tank (time step $\Delta t = 0.04$ s).

The surge tank water level oscillations are shown in Fig. 9. The maximum water level in the surge tank occurred at time $t = 114$ s and it is 623 m; much lower than the overflow elevation of 628 m. Minimum water level in the surge tank occurred at the time $t = 223$ s and it is equal to 585 m. There is no danger of surge tank emptying for the case considered because the surge tank

bottom is at elevation of 577.5 m i.e. the minimum water level is 7.5 m above surge tank bottom level. Only a small discrepancy in the phase shift occurs after $t = 360$ s. Numerical models show better agreement with the results of measurements than for the flow situation in the downstream end of the junction (Figs. 7 and 8).

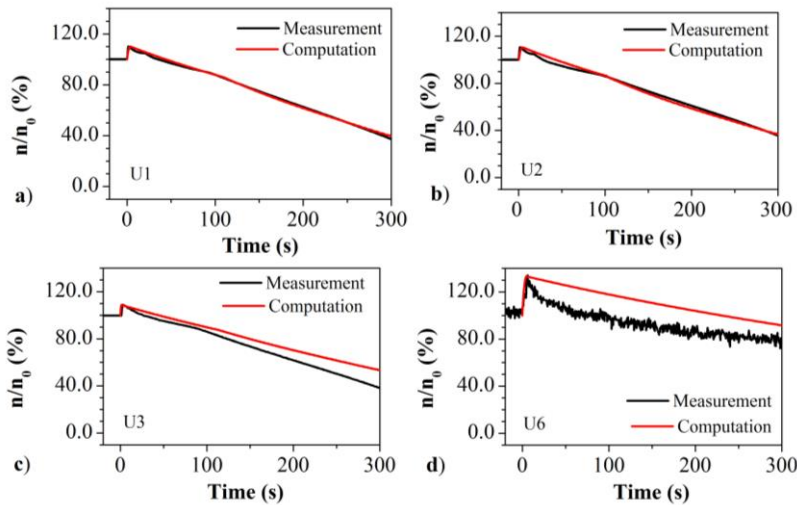


Fig. 10. Rotational speed change ($n_0 = 375$ min $^{-1}$, U1, U2, U3 and $n_0 = 428$ min $^{-1}$, U6) during plant emergency shut-down from $P_0 = 303.54$ MW

Fig.10 shows comparison between the computed and measured turbine rotational speed changes for Units 1, 2, 3 and 6. The maximum measured and calculated turbine speed rise for all units occurs at time $t = t_{def}$ where t_{def} is jet deflector operating time. The computed maximum turbine rotational speed rise matches the maximum measured value for all units (Fig. 10). After the jet deflector deflects the water into the tailrace the turbine speed decrease is influenced only by the dissipation torques

because the turbine wheel is not affected by the hydraulic torque. For the first four units (U1 to U4), that have been already refurbished, the maximum turbine speed rise is about 10% and well below the permissible speed rise of 25%. For the un-refurbished units (U5 to U7) the speed rise is of the same magnitude as the permissible one. Refurbishment of worn out units is foreseen in the near future. The discrepancies between the calculated and measured rotational speed time

histories are higher for the U6 and it is attributed to larger bearing and ventilation losses.

4 CONCLUSIONS

New in-situ experimental and computed results for the case of simultaneous emergency shut-down of seven Pelton turbines in a high-head hydropower plant Perućica, Montenegro are presented. The experiment has been performed at very high Reynolds number flows (larger than 10^7) not reported in the open literature. The in-house numerical algorithm is based on the method of characteristics where the frictional losses are modelled by using the QSF (standard quasi-steady friction) and the CBM (convolution-based unsteady friction) models. The algorithm first computes water hammer in the fluid conveyance system and then separately the turbine rotational speed rise by using the results from the first step. The turbine model takes into account friction losses in the shaft bearings and ventilation losses in the turbine housing [6]. From comparisons of head changes at the downstream end of the penstocks it can be seen that CBM gives only a little better results. It can be concluded that inclusion of unsteady friction into numerical models is not necessary when relatively slow transients are considered at initially high Reynolds number flows (10^6 [6] to 10^7 (this paper)). In addition, the model simulates the changes of the water level in surge tank accurately. During power plant shut-down there will be no spillage of water from the surge tank overflow nor surge tank emptying and air inflow into concrete tunnel. When it comes to the units' speed change, the numerical results agree well with the results of measurements for the refurbished units. The discrepancies between the results for the worn out units are larger due to increased dissipation torques. It may be concluded that the developed numerical model gives good agreement with the results of measurements and as such it is recommended for the use in engineering practice for hydropower plants with Pelton turbines.

5 ACKNOWLEDGEMENTS

The authors gratefully acknowledge Institute Jaroslav Černi and members of the Electric Power Supply Company Modernization

team for the authorization to publish results obtained during measurement campaign. Support of the Slovenian Research Agency (ARRS) and the Ministry of Science of Montenegro (MSM) conducted through the project BI-ME/14-15-016 (ARRS, MSM) and the programme P2-0162 (ARRS) is acknowledged as well.

6 REFERENCES

- [1] Arrington, R. M. (1999). Failure of water-operated needle valves at Bartlett Dam and Oneida station hydroelectric plant. *Proc. 3rd ASME/ JSME Joint Fluid Engineering Conference*, San Francisco, California, USA, p. 385-390.
- [2] Adamkowski, A. (2001). Case study: Lapino powerplant penstock failure. *ASCE J. Hydraul. Eng.*, vol. 127, no. (7), p. 541-555, DOI:10.1061/(ASCE)07339429(2001)127:7(547).
- [3] Russell, W. R. (2010). Restoring Sayano-Shushenskaya. *HRW-Hydro Review Worldwide*, vol. 18, no. 1, p. 12-20.
- [4] Bissel, C., Vullioud, G., Weiss, E., Heimann, A., Chene, O., Dayer, J.-D. and Nicolet, C. (2011). Recommissioning of the Bieudron powerplant. *The International Journal on Hydropower & Dams*, vol. 18, no. 3, p. 82-85.
- [5] Vereide, K., Svingen, B., and Guddal, R. (2015). Case study: Damaging effects of increasing the installed capacity in an existing hydropower plant. *Proceedings of the 12th International Conference on Pressure Surges*, BHR Group, Dublin, Ireland, p. 417-424.
- [6] Karadžić, U., Bergant, A., and Vukoslavčević, P. (2009). A novel Pelton turbine model for water hammer analysis. *Strojniški Vestnik – Journal of Mechanical Engineering*, vol. 55, no. 6, p. 369-380.
- [7] Wylie, E. B., and Streeter, V. L., (1993). *Fluid Transients in Systems*, Prentice Hall, Englewood Cliffs, USA.
- [8] Chaudhry, M.H. (2014). *Applied hydraulic transients*, Springer, New York, USA. DOI:10.1007/978-1-4614-8538-4.
- [9] Zielke, W. (1968). Frequency-dependent friction in transient pipe flow. *ASME J. Basic Eng.*, vol. 90, no. 1, p. 109-115, DOI:10.1115/1.3605049.
- [10] Vardy, A.E., and Brown, J.M.B. (2003). Transient turbulent friction in smooth pipe flows. *Journal of Sound and Vibration*, vol. 259, no. 5, p. 1011-1036, DOI:10.1006/jsvi.2002.5160.

- [11] Vitkovský, J., Bergant, A., Simpson, A., and Lambert, M. (2006). Systematic evaluation of one-dimensional unsteady friction models in simple pipelines. *ASCE J. Hydraul. Eng.*, vol. 132, no. 7, p. 696-708, DOI: 10.1061/(ASCE)0733-9429(2006)132:7(696).
- [12] Adamkowski, A., and Lewandowski, M. (2006). Experimental examination of unsteady friction models for transient pipe flow simulation. *ASME Journal of Fluids Engineering*, vol. 128, no. 6, p. 1351–1363, DOI: 10.1115/1.2354521.
- [13] Riasi, A., Raisee, M., and Nourbekhsh, A. (2010). "Simulation of transient flow in hydroelectric power plants using unsteady friction. *Strojniški vestnik – Journal of Mechanical Engineering*, vol. 56, no. 6, p. 377-384.
- [14] Duan, H.-F., Ghidaoui, M.S, Lee, P.J., Tung, Y.K. (2012). Relevance of unsteady friction to pipe size and length in pipe fluid transients. *ASCE J. Hydraul. Eng.*, vol. 138, no. 2, p. 154-166, DOI:10.1061/(ASCE)HY.1943-900.0000497.
- [15] Meniconi, S., Duan, H.F., Brunone, B., Ghidaoui, M.S., Lee, P.J. and Ferrante, M. (2014). Further developments in rapidly decelerating turbulent flow modelling. *ASCE J. Hydraul. Eng.*, vol. 140, no. 7, p. 1-9, DOI: 10.1061/(ASCE)HY.1943-7900.0000880.
- [16] Vardy, A.E. (2018). Acceleration-dependent unsteady friction revisited. *Proceedings of the 13th International Conference on Pressure Surges*, BHR Group, Bordeaux, France, p. 265 - 282.
- [17] Trikha, A.K. (1975). An efficient method for simulating frequency-dependent friction in transient liquid flow. *Journal of Fluids Engineering*, ASME, vol. 97, no. 1, p. 97 – 105, DOI: [10.1115/1.3447224](https://doi.org/10.1115/1.3447224).
- [18] Zarzycki, Z. (1997). Hydraulic resistance of unsteady turbulent liquid flow in pipelines. *Proceedings of the 3rd International Conference on Water Pipeline Systems*, BHR Group, The Hague, The Netherlands, p. 163 - 178.
- [19] Vardy, A.E., and Brown, J.M.B. (2004). Transient turbulent friction in fully rough pipe flows. *Journal of Sound and Vibration*, vol. 270, no. 1-2, p. 233-257, DOI:10.1016/S0022-460X(03)00492-9.
- [20] Vitkovský, J., Stephens, M., Bergant, A., Lambert, M., and Simpson, A. (2004). Efficient and accurate calculation of Zielke and Vardy-Brown unsteady friction in pipe transients. *Proceedings of the 9th International Conference on Pressure Surges*, BHR Group, Chester, UK, p. 405-419.
- [21] Urbanowicz, K. (2017). Analytical expressions for effective weighting functions used during simulations of water hammer. *Journal of Theoretical and Applied Mechanics*, vol. 55, no. 3, p. 1029–1040, DOI: 10.15632/jtam-pl.55.3.1029.
- [22] Urbanowicz, K. (2018). "Fast and accurate modelling of frictional transient pipe flow. *Zeitschrift für Angewandte Mathematik und Mechanik*, vol. 98, no. 5, p. 802-823, DOI: 10.1002/zamm.201600246.
- [23] Starinac, D., Džopalić, D., Predić, Z., Gajić, A., Vojt, P., and Dimitrijević, M. (2011). Final report on in-situ measurement campaign at Perućica HPP, Montenegro – Part 2: Pressurized system. *Jaroslav Černi Institute for the Development of Water Resources (JCI)*, Belgrade, Serbia.
- [24] Starinac, D., Žugić, D., Predić, Z., Gajić, A., Džopalić, D., and Vojt, P. (2012). In-situ measurement campaign at the Perućica hydropower plant in Montenegro - Part 2: Pressurized system. *Water Research and Management*, vol. 2, no. 4, p. 3-17.
- [25] Nicolet, C., Vulllioud, G., Weiss, E., Bocherens, E., Dayer, J.-D. and Chene, O. (2012). Transient analysis of Cleuson-Dixence power plant and injector closure in the reflection time. *Proceedings of the 11th International Conference on Pressure Surges*, BHR Group, Lisbon, Portugal, p. 27-41.